A Combined Electromagnetic and Thermal Approach to the Design of Electrical Machines

D. G. Dorrell*, D. A. Staton** and M. I. McGlip*
* Dept of Electronics and Electrical Engineering, University of Glasgow, Glasgow, UK
** Motor Design Ltd, Ellesmere, Shropshire, UK

***Abstract*—This paper reports on methods for the analysis of electrical machines by combined electromagnetic and thermal models using commercial software which can be an aid to the design of these machines. Examples using a brushless permanent-magnet motor and an induction motor illustrate the tools available and techniques possible.**

***Index Terms*—Thermal analysis, electromagnetic design, motors**

I. INTRODUCTION

The thermal modelling of electrical machines is not a straightforward issue. It is very much a function of the manufacturing procedures and environment in addition to the cooling system in implemented. A machine that is correctly mounted on a heat-sinking plate or pedestal with the correct airflow around it is obviously going to less liable to overheating when compared to a poorly fitted machine in a high-ambient sealed enclosure. In addition the load duty cycle will have an effect. A machine may operate correctly for a short time before thermal overload; therefore a machine should be rated according to several different duty cycles for full rating specification.

There are obvious outcomes to thermal overload. The windings may begin to burn out due to excessive temperatures and permanent demagnetization may occur in magnets if it is a permanent-magnet machine.

Two recent papers [1][2] on the thermal performance of a brushless permanent magnet motor illustrated that it is possible, with careful attention to the manufacturing techniques used to produce the machine, and the associated thermal resistances and capacitances, to obtain good steady-state and transient thermal performance prediction. Often the electromagnetic design is carried out using known parameters that should not be exceeded (e.g., a maximum winding current density of 5 to 7 A/mm^2) then the thermal design is carried out once the electromagnetic design has been set. The thermal design then has set losses that can be used in a thermal network.

The thermal considerations for a permanent magnet motor can be straightforward compared to other electrical machines since the current is usually controlled, so that the copper loss can be easily assessed if the temperature and ambient-temperature winding resistance are known. An iterative procedure can then be implemented to calculate the machine temperatures as well as other parameters (such as magnet demagnetizing) to reach either a steady-state temperature set or a transient temperature curve set.

Voltage-fed machines, such as the induction motor, are more difficult to assess in terms of their thermal performance. Especially since a direct on-line start is actually a transient over-load; the stator and rotor currents are many times the steady-state ratings. If a motor has a starting problem (i.e., it is locked) then the machine can quickly overheat. It would be hoped that the fusing of the machine would be correct so that the transient over-current will break the circuit before damage occurs. However, if the duty cycle of the machine requires many stop-start cycles then the motor may be starting from hot.

In addition, the starting performance will vary according to the induction motor temperature.

The thermal rating will be affected by the cooling. For instance, many general purpose induction motors are simple totally-enclosed fan-cooled machines. However, specialist machines, such as those incorporated in down-hole pumps, may have much better cooling, with cans on the stator and/or rotor and fluid-filled air-gaps to aid rotor cooling and lubricate bearings. These machines will often use the water they are pumping to cool the stator casing.

In this paper, an electromagnetic-thermal link approach to motor analysis will be taken to assess the performance of an induction motor in terms of its starting transient behaviour. First, the software link is verified using results from the brushless permanent magnet study conducted in [1] and [2].

II. VERIFICATION OF SOFTWARE – PERMANENT MAGNET MOTOR STUDY

The modelling approach is first verified using a brushless permanent magnet motor. The machine was tested with several thermocouples to measure the motor temperature over a period of time and with several cycles. The software used in the simulation was *SPEED* PC-BDC (as developed by The *SPEED* Laboratory, University of Glasgow, UK), which is a specialist electromagnet design package for brushless permanent-magnet machines, and MotorCAD (developed by Motor Design Ltd, UK) which is a specialist thermal design package for electrical machines. Both of these packages run under the Window environment and are linked via a special routine that unitizes the Windows ActiveX facilities (often called COM). PC-BDC does have several

This work is supported by Grundfos Management Systems, Denmark (who supplied details of the induction motor) and the thermal measurements were taken by Mr Piotr Holik. The authors are grateful for their assistance.

thermal analyses routines. Indeed the most sophisticated node model in PC-BDC has ten thermal nodes so it is quite sophisticated in its own right in terms of thermal modelling. However, MotorCAD is totally dedicated to thermal analysis and offers a model with over 35 nodes and gives great assistance in helping the designer to realize the correct thermal model by interpreting different manufacturing techniques commonly used in motor manufacture and allocating the correct thermal resistance or capacitance to each component. Naturally there are many adjustment factors available with MotorCAD (as there is in PC-BDC).

A. Motor Design for Brushless Motor

The machine cross section is shown in Fig. 1 as denoted in PC-BDC. The axial section, as illustrated by MotorCAD is shown in Fig. 2. The full details of the machine are given in [1] and [2]. An actual photograph of this machine is shown in Fig. 3. It should be noted that all the experiments were conducted at 2600 rpm. This machine was an AC machine, so that to allow for full-current operation without the need to attach a load, then the encoder was rotated so that the machine would run at full current but produce only enough torque to maintain the speed without a load.

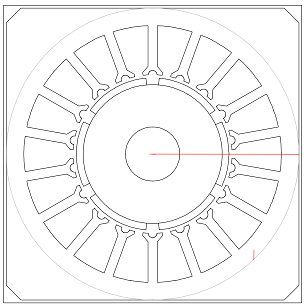

Fig.1. Brushless permanent magnet motor cross section in PC-BDC

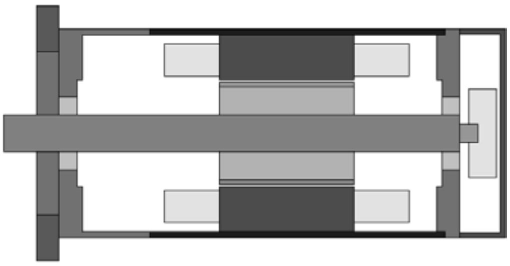

Fig. 2. Axial section in MotorCAD

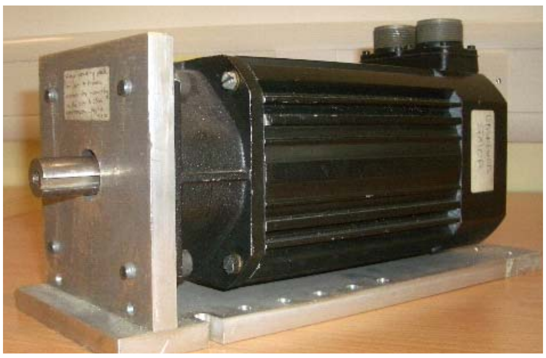

Fig. 3. Actual brushless permanent magnet motor

B. Transient Simulations

Using the MotorCAD-SPEED link transients simulations were carried out and these were repeated experimentally for the machine. Fig. 4 shows the comparison between the measured and simulated temperatures for the machine as described in [1] over a cycling load between full load current at 2600 rpm and standstill (when off and cooling). The left-hand legend results are simulated, while the right-hand are measured. It can be seen that the internal motor temperatures match well (layer [4] indicated the layer of conductor in the stator slot because there is a temperature gradient from the centre of the coil to the outer layer of the coil). The shaft temperature was only measured when stationary using a temperature probe and the divergence between the shaft temperatures is considered to be due to the use of this uncalibrated probe. A more detailed study of the thermal modelling considerations of this machine are given in [1] and [2].

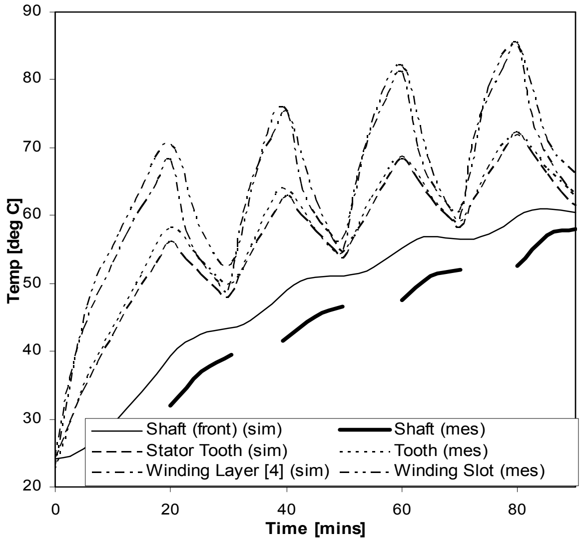

Fig. 4. Comparison between measured and simulated temperatures in the brushless permanent machine

III. INDUCTION MOTOR MODELLING

The package was further used to simulate the behaviour of a 3-phase induction motor. This machine is used in a water pump and has been designed explicitly for this application. The stator is totally enclosed with a stainless steel casing and a stainless steel internal can. The air-gap is fluid-filled for cooling and also bearing lubrication. Usually the smooth casing is water cooled although this was not carried out for the locked-rotor tests where the motor was removed from the pump unit. This time the *SPEED* induction motor design package PC-IMD was used in conjunction with MotorCAD.

A. Motor Specification

The test machine is a 2-pole copper-cage machine. It is a 400 V 3-phase 2.2 KW submersible motor. The cross-section is shown in Fig. 5. The rotor has 1.33 stator slot skew and the cage is copper. This machine has been examined in detail for its performance in terms of inter-bar current in [3] and [4]. However, here, the PC-IMD design uses the inter-bar resistance facility developed within the software [5] bring the small discrepancies between the simulation and measured performances into agreement. This was carried out using the low voltage measurements where the saturation is low. There will be variation at high voltage due to axial saturation [4] although this is not greatly different, and the 400 V (rated voltage) simulations should be sufficient to highlight the variation of the performance with temperature. The PC-IMD model was kept constant through the whole of the simulations here.

The PC-IMD cross-section is shown in Fig. 5 while the axial section from MotorCAD is shown in Fig. 6. It can be seen that this is a long machine.

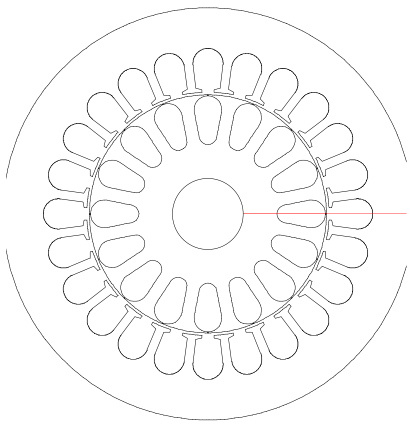

Fig. 5. PC-IMD cross section for induction motor

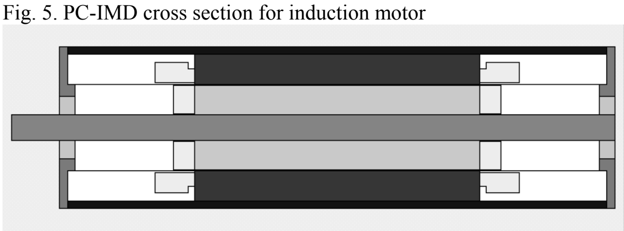

Fig. 6. MotorCAD axial section for induction motor

B. *Low Voltage Simulation and Verification at Locked Rotor*

The machine was tested at 90 V over a period of time and locked rotor conditions to verify the transient temperature rise. The machine was first tested with the variation of locked rotor position at ambient temperature. This is because it was found in [4] that there was a variation in locked rotor torque. These results are illustrated in Fig. 7 for three separate measurements. It was first measured for one example machine by the manufacturer. Another example of this machine was also tested in The University of Glasgow. This was measured twice to ensure that static friction had no effect. The torque was first measured while moving the rotor from 0º to 24º (at 3º intervals) using a dividing head to hold the rotor. It was then measured while moving the rotor in the opposite direction (without changing the phase rotation). It was found that the mean torque for the manufacturer-tested machine was 0.47 Nm while the two University-tested machine characteristics gave an average locked rotor torque of 0.5 Nm. This spread is typical for this machine [3]. The inter-bar resistance was adjusted in PC-IMD to give the correct locked rotor torque. It was then found there was excellent phase current and good input power correlation.

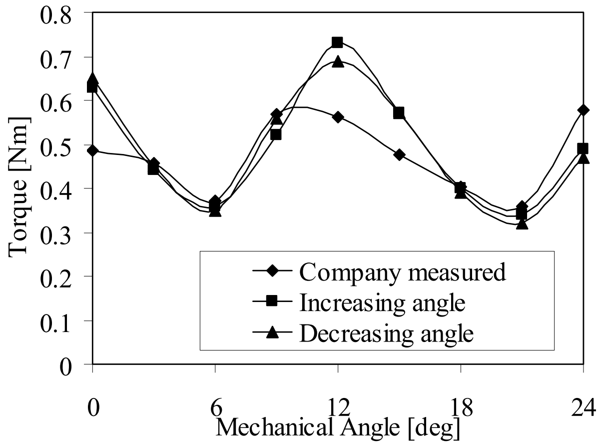

Fig. 7. Variation of locked rotor torque at 90 V and ambient temperature

The temperature was then measured over a six minute period. Two measurement points were used. One was on the stator casing at the halfway point down the axial casing length. The second measured the temperature inside the machine on the rotor surface above a bar.

The MotorCAD/PC-IMD link simulations were set using a MATLAB script that controlled the time steps and number of simulation points. This is because at each step the temperature has to be calculated and then the current recalculated until a power-balance/temperature equilibrium is obtained. A number of points are used between each time step to ensure a steady incremental temperature variation. At low voltage a time step of 10 sec was used with three intermediate calculation points. These are shown in Fig. 8. Any node can be tracked however here we show the variation of casing temperature (which should track the measured casing temperature) and the bar temperature (which should track a temperature just above the measured rotor surface temperature). This is shown to be the case so that the good agreement was found with a 10 second time step.

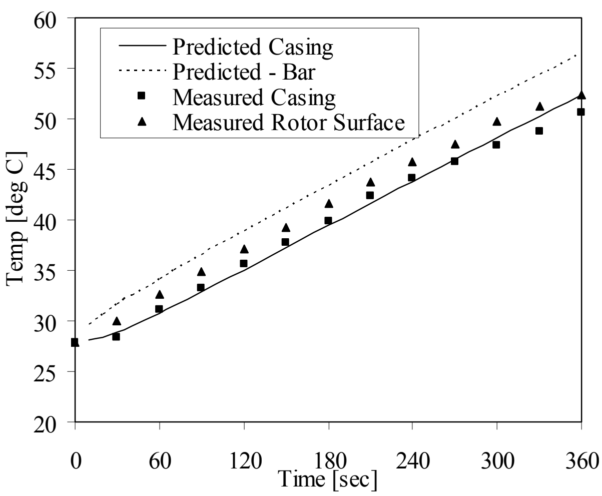

Fig. 8 Comparison between measured and simulated temperatures

The variation of measured and simulated input power and phase current are shown in Fig. 9. These illustrate the good correlation without having to adjust factors (apart from inter-bar resistance) to obtain precise prediction.

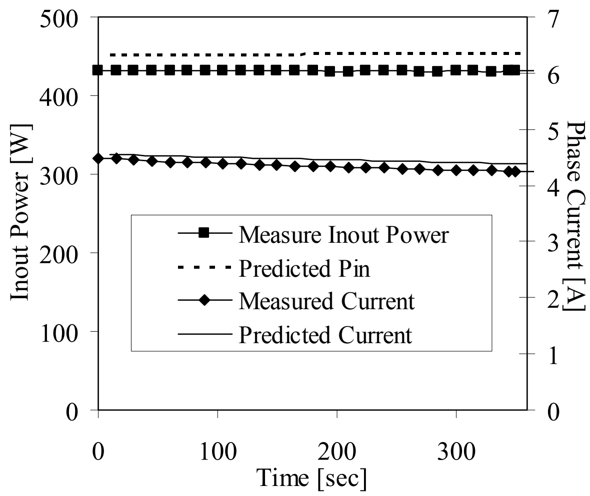

Fig. 9. Comparison between the measured and predicted input power and phase currents at 90 V

C. Rated Voltage Simulation at Locked Rotor

The machine was then simulated over a 30 sec period with 1 second time intervals to investigate the thermal stability of the machine at 400 V and locked rotor. Since the machine has simple natural cooling with air surrounding the casing in the laboratory then it was found that the machine heated up rapidly. The temperature predictions are shown in Fig. 10. It can be seen that while the casing temperature increases slowly, the winding temperature increases rapidly and with 30 seconds will exceed even a Class F insulation rating.

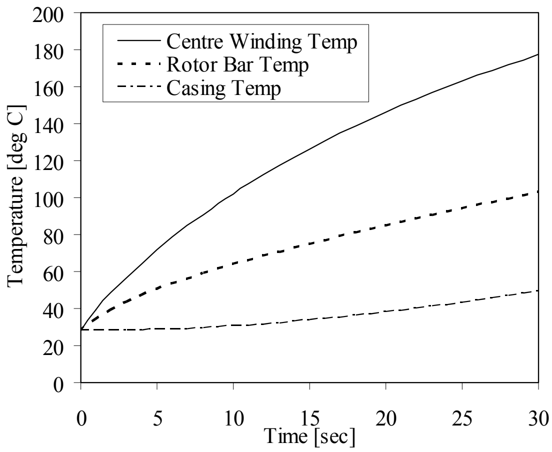

Fig. 10. Temperature simulations at locked rotor and rated 400 V

The input current is shown in Fig. 11 and the torque and input power predictions are shown in Fig. 12. These illustrate the transient has is relatively fast changing if a measurement is being attempted without the use an automated measurement system or a date logging power analyzer and torque transducer. The current changes from 21.9 A to 18.3 A, the input power changes from 10.6 kW down to 9.9 kW while the torque changes from 11.8 down to 9.6 Nm.

There is a minor perturbation in the results which illustrates the iterative nature of the calculation routines. The locked rotor torque was measured to be about 11.5 Nm for this design under cold conditions across several different machines during an automated torque-speed curve test [4]. A further locked-rotor test measured the torque to be 13.3 Nm and it was hypothesized that this may be due to thermal variations in the different measurement techniques. However, it appears that it may simply be an error in the measurement reading that leads to an over-estimation.

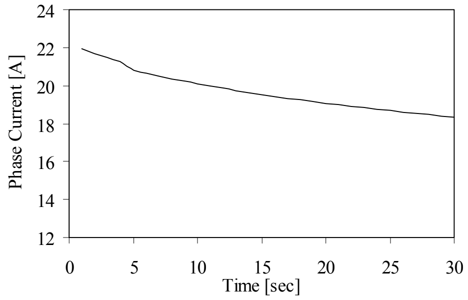

Fig. 11. Phase current prediction at locked rotor and rated 400 V

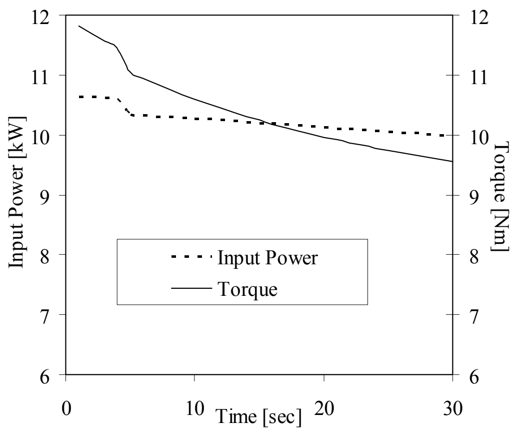

Fig. 12. Input power and torque predictions at locked rotor and rated 400 V

D. Transient at Rated Speed and Air Cooling

The machine was now simulated at full voltage at the rated speed of 2883 rpm. The temperature variations calculated over ten minutes are shown in Fig. 13 and the temperatures are still low but still rising steadily. Therefore steady-state is still some way off. In Fig. 8 it can be seen that the measured temperature results do seem to be exhibiting some curvature after four minutes – showing that there is more air cooling around the machine than incorporated in the simulation. Obviously within a laboratory situation there is natural movement of the air around the machine due to air-conditioning and ventilation. This can be refined further if necessary though it is not regarded as necessary here since we are illustrating the combined electro-magnetic/thermal modelling approach and the ease with which reasonable results can be obtained without fine tuning after experimental results have been obtained. The final steady-state predicted temperatures are 266 ºC for the winding, 257 ºC for the rotor bar and 252 ºC for the casing; this indicates the poor nature of the air cooling over the smooth stainless-steel stator casing. In the next section water cooling will be introduced.

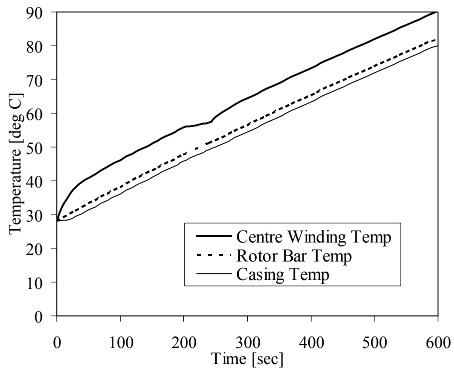

Fig. 13. Temperature variation over 10 minutes at 400 V and 2886 rpm

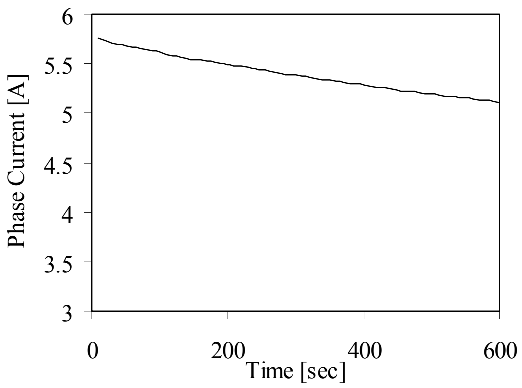

Fig. 14. Phase current variation over 10 minutes at 400 V and 2886 rpm

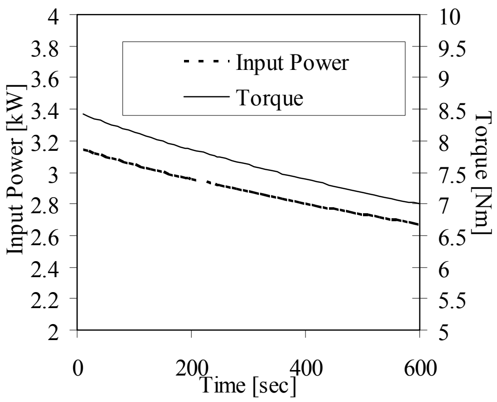

Fig. 15. Input power and torque over 10 minute at 400 V and 2886 rpm

The phase current is shown in Fig. 14 and the torque and input power are shown in Fig. 15. These illustrate a steady change but not the high change at rated speed so that experimental results can be obtained at rated speed and full voltage in the laboratory, where full cooling is not present. After ten minutes the toque is predicted to be 7 Nm which is 2.1 kW of mechanical power at 2883 rpm showing this is actually slightly below the rated value. This illustrates that the machine runs quite cool since is it water cooled.

E. Transient at Rated Voltage and Speed with Water Cooling

The machine, when tested in the laboratory, does not have the same level of cooling compared to when it is fitted and operating in a water pump. If we surround the stator with water in the simulation then we now obtain good cooling. The final steady-state predicted temperatures are 47.7 ºC for the winding, 38.6 ºC for the rotor bar and 34.1 ºC for the casing, when the water temperature is set at 28 ºC. The torque is 8.1 Nm which corresponds to a torque of 2.45 kW (excluding the mechanical torque loss due bearing and air-gap fluid friction). The transient temperatures are shown in Fig. 16. This illustrates that the operation of this motor is very dependant on the cooling arrangement of the machine.

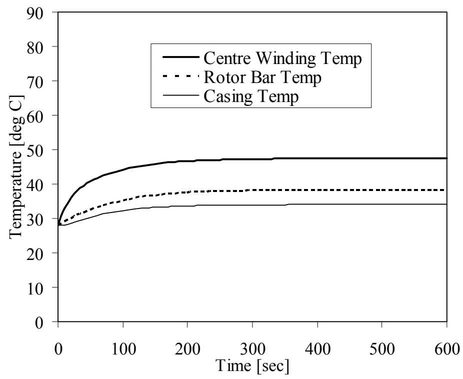

Fig. 16. Temperature variation over 10 minutes at 400 V and 2886 rpm with external casing water cooling

F. Torque/Speed Curve Simulation

To test an induction motor the machine is often put on to a test rig which will run the machine up to synchronous speed then apply the terminal voltage and load the machine in a controlled manner that reduces the speed down to standstill, then possibly run it back to synchronous speed. While this is taking place various parameters can be logged such as input current, input power, power factor and torque. This should be a steady-state test so that the test period will have a time period of a few seconds to prevent transient effects.

The MotorCAD/PC-IMD Link, when scripted through a MATLAB program, can simulate this. Fig. 17 shows the temperature simulation over a 20 second measurement where the motor is run down to standstill then back up to synchronous speed. The torque/speed and current/speed curves are shown in Figs. 18 and 19. These clearly illustrate that the torque/speed curve should be obtained as quickly as possible when carried out at full voltage. This can be illustrated by decreasing the time to 10 seconds. This is shown in Fig. 20. The peak temperature at the end of the test is now predicted to be 79 ºC rather than 110 ºC.

If the system is good and the data can be acquired quickly then we can reduce the test time even further and the torque/speed curve for a 5 second test is shown in Fig. 21 showing an even greater improvement in the torque/speed curve consistency. The peak winding temperature is further reduced to 60 ºC.

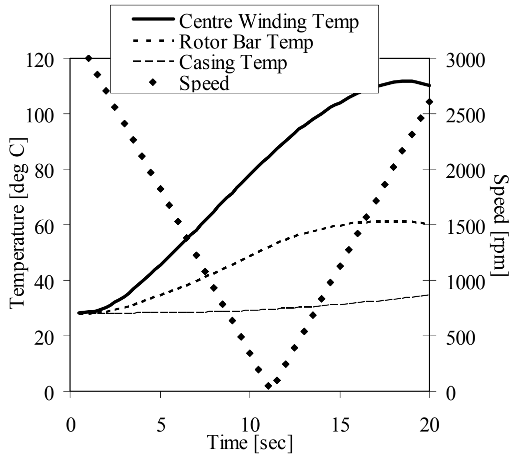

Fig. 17. Variation of temperature with time for a torque/speed curve at 400 V

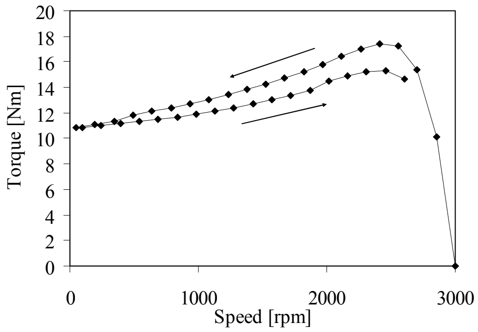

Fig. 18. Torque/speed curve over 20 second test at 400 V

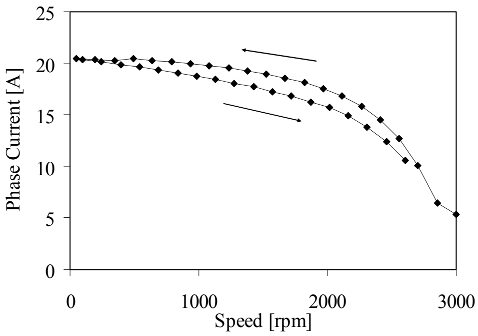

Fig. 19. Current/speed curve over 20 second test at 400 V

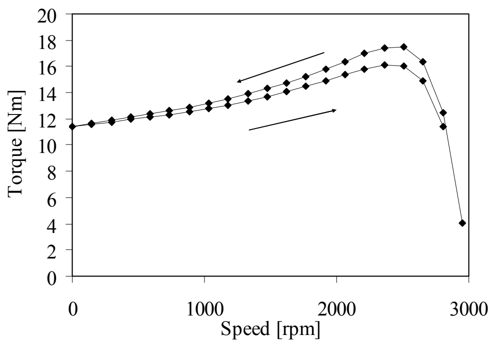

Fig. 20. Torque/speed curve over 10 second test at 400 V

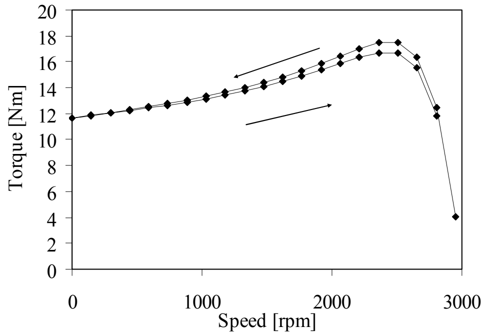

Fig. 21. Torque/speed curve over 5 second test at 400 V

G. Discussion

The simulation results in this section illustrate that combined electromagnetic-thermal analysis of an electrical machine can be incorporated into the design procedure to account for duty cycling, and to incorporate the correct thermal system and rate the cooling correctly. It has been used here to help in the interpretation of induction motor testing and has been verified with temperature monitoring in a reduced-voltage locked-rotor test. In the previous section it was also illustrated to work when analyzing a brushless permanent magnet motor.

IV. Conclusions

This paper illustrates that thermal modelling of an electrical machine is very important in the design procedure and performance simulation. It also shows that more complete design and analysis is possible using modern CAD packages and these packages can be linked together. The method was first verified using a brushless permanent magnet motor then further used to validate the thermal behaviour of a 3-phase induction motor to illustrate the transient nature of the machine performance at standstill and in the measurement of the torque/speed curve.

References

[1] D. G. Dorrell, D. A. Staton, J. Kahout, D. Hawkins and M. I. McGilp, "Linked Electromagnetic and Thermal Modelling of a Permanent Magnet Motor", *IEE Power Electronics, Machines and Drives Conference*, Dublin, April 2006.

[2] D. G. Dorrell, D. A. Staton and M. I McGilp, "Design of Brushless Permanent Magnet Motors – A Combined Electromagnetic and Thermal Approach to High Performance Specification," *IEEE IECON Conference*, Paris, France, Nov 7 – 10, 2006.

[3] D. G. Dorrell, P. J. Holik, H.-J. Thougaard, F. Jensen and P. Lombard "Modelling Axial Variations in Induction Motors with Rotor Skew using Multi-sliced 2D Finite Element Analysis*", IEE Power Electronics, Machines and Drives Conference* PEMD, Dublin, Ireland, April 2006.

[4] P. J. Holik, D. G. Dorrell, P. Lombard, H.-J. Thougaard and F. Jensen, "A Multi-Sliced Finite Element Model for Induction Machines Incorporating Inter-bar Current", *IEEE IAS Conference*, Tampa, Florida, USA, October 2006.

[5] D. G. Dorrell, TJE Miller and C. B. Rasmussen, "Inter-bar Currents in Induction Motors", *IEEE Trans on Industry .Applications*, Vol. 39 No 3 pp 677-684, 2003.